Effects of Weakly Nonlinear Water Waves on Soft Poroelastic Bed with Finite Thickness

Ping-cheng Hsieh[1] and Liang-hsiung Huang, A.M.ASCE[2]

Abstract: Since porous material is usually of a finite thickness in nature, the effects of periodically nonlinear water waves propagating over a soft poroelastic bed with finite thickness are hence noticed and studied in this work. The water waves are simulated by potential theory while the porous bed is governed by Biot's theory of poroelasticity herein. The conventional Stokes expansion of water waves based on a one-parameter perturbation expansion fails to solve the soft poroelastic bed problem; therefore, the boundary layer correction approach combined with a two-parameter perturbation expansion is proposed, which enables us to solve the problem of soft poroelastic bed with finite thickness. The results are compared to the similar problem with an infinite-thickness porous bed. The boundary effects of the impervious rock are significant on wave-induced pore water pressure and effective stresses, but are of very little significance on wave profiles at the free surface and the porous bed surface. However, the rigid boundary is insignificant to the pore water pressure and effective stresses when the thickness of porous bed is larger than about one wavelength.

DOI: 10.1061/(ASCE)0733-9399(2003)129:2(210)

CE Database keywords: Water waves; Boundary processes; Beds; Thickness.

Introduction

The dynamic response of a propagating water wave acting on coastal constructions is quite emphasized during the design work especially in the analysis of seabed instability. The wave-induced variation in pore pressure and effective stresses has been recognized as a major factor for destroying the stability of the seabed so that it is very important to correctly estimate the pore pressure and effective stresses inside the seabed.

At the early stage, most researchers only study the linear or nonlinear water waves acting on a seabed that was usually assumed to be rigid material; yet, it was considered as permeable (Putnam 1949; Reid and Kajiura 1957; Sleath 1970; Moshagen and Torum 1975) or impermeable (Mei 1983; Fenton 1985; Dean and Dalrymple 1991). Actually, fluid within the porous material interacting with a deforming solid skeleton is very obvious and, thus, a realistic analysis based on deformable porous seabed is necessary.

Biot (1956) developed a theory of poroelasticity to discuss the elastic wave in a fluid-saturated porous solid. Huang and Chwang (1990) investigated Biot's oscillatory equation for an acoustic problem without simplifications and obtained three decoupled Helmholtz equations standing for three kinds of wave—two longitudinal waves and one transverse wave. Following this method, Huang and Song (1993) then analytically solved the problem of periodically linear water waves interacting with a deformable bed by treating the bed as a poroelastic material. Their approach was quite successful in revealing most physical mechanisms by using a potential water wave and Darcy's porous medium flow. Chen et al. (1997) further applied the conventional Stokes expansion of a nonlinear deepwater wave based on $\varepsilon_1 = k_0 a$ to investigate the dynamic response of a deformable permeable seabed. They found that the Stokes expansion is only valid for the hard poroelastic material but invalid for the soft one even though the Ursell parameter is small. Finally, Hsieh et al. (2000) proposed a two-parameter perturbation method and a boundary layer correction approach to carry out the analytic solution of nonlinear water waves propagating over a soft poroelastic material bed with infinite thickness. Note that Huang and Song (1993), Chen et al. (1997), and Hsieh et al. (2000) all focused on a poroelastic bed with an infinite thickness.

Based on the fact that the seabed is generally multilayered and the nonlinear water waves are very likely to happen, the present study will find a way to investigate the complicated finite depth problem and the interaction between the nonlinear water waves and the poroelastic material seabed with a single layer, i.e., the thickness of the porous bed is finite. The present work is aimed at investigating the boundary effect of a soft poroelastic seabed under periodically nonlinear water waves propagation.

Mathematical Formulation

The plane water waves, as indicated in Fig. 1, propagating over a horizontally finite-thickness homogeneous poroelastic bed, are simulated by the potential theory and the porous medium saturated with water is governed by Biot's theory of poroelasticity (1956). Region (1) ranges from $y=\xi^*(x,t)$ to $y=h+\eta^*(x,t)$; and region (2) from $y=\xi^*(x,t)$ to $y=-B$. Symbols η^* and ξ^*=the displacements of waves from the mean-free surface ($y=h$) and the mean surface of porous bed ($y=0$), respectively.

[1]Assistant Professor, Dept. of Soil and Water Conservation, National Chung-Hsing Univ., Taichung, 40227, Taiwan, ROC (corresponding author). E-mail: pchsieh@dragon.nchu.edu.tw

[2]Professor, Dept. of Civil Engineering, National Taiwan Univ., Taipei, 106, Taiwan, ROC.

Note. Associate Editor: Keh-Han Wang. Discussion open until July 1, 2003. Separate discussions must be submitted for individual papers. To extend the closing date by one month, a written request must be filed with the ASCE Managing Editor. The manuscript for this paper was submitted for review and possible publication on March 14, 2001; approved on July 1, 2002. This paper is part of the ***Journal of Engineering Mechanics***, Vol. 129, No. 2, February 1, 2003. ©ASCE, ISSN 0733-9399/2003/2-210–222/$18.00.

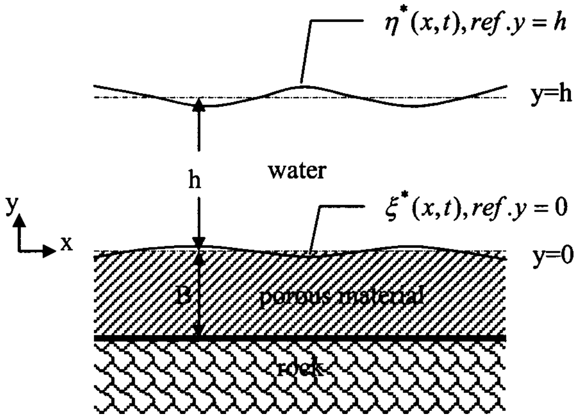

Fig. 1. Definition sketch

Boundary-Value Problem

Assuming that the homogeneous flow, region (1) of Fig. 1, is potential flow, the velocity $\underline{u}^{*(1)}$ can be represented by velocity potential $\Phi^{*(1)}$ as

$$\underline{u}^{*(1)}=\nabla\Phi^{*(1)} \tag{1}$$

The equations of continuity and momentum in terms of velocity potential hence become

$$\nabla^2\Phi^{*(1)}=0 \tag{2}$$

$$\rho_0\frac{\partial\Phi^{*(1)}}{\partial t}+\frac{\rho_0}{2}\left\{\left[\frac{\partial\Phi^{*(1)}}{\partial x}\right]^2+\left[\frac{\partial\Phi^{*(1)}}{\partial y}\right]^2\right\}+P^{*(1)}=0 \tag{3}$$

where $P^{*(1)}$=the wave-induced pressure in region (1), and ρ_0=the density of water.

Referring to Huang and Chwang (1990), the linear momentum equations of a solid skeleton and fluid for the porous bed based on the theory of poroelasticity may be written as

$$\nabla\cdot\underline{\underline{\sigma}}^{*}=\rho_{11}\frac{\partial^2\underline{d}^{*}}{\partial t^2}+\rho_{12}\frac{\partial^2\underline{D}^{*}}{\partial t^2}+b\left(\frac{\partial\underline{d}^{*}}{\partial t}-\frac{\partial\underline{D}^{*}}{\partial t}\right) \tag{4}$$

$$\nabla\cdot\underline{\underline{S}}^{*}=\rho_{12}\frac{\partial^2\underline{d}^{*}}{\partial t^2}+\rho_{22}\frac{\partial^2\underline{D}^{*}}{\partial t^2}-b\left(\frac{\partial\underline{d}^{*}}{\partial t}-\frac{\partial\underline{D}^{*}}{\partial t}\right) \tag{5}$$

with

$$\underline{\underline{\sigma}}^{*}=\underline{\underline{\tau}}^{*}-(1-n_0)P^{*(2)}\underline{\underline{I}} \tag{6}$$

$$\underline{\underline{\tau}}^{*}=2G\underline{\underline{e}}^{*}+\lambda(\nabla\cdot\underline{d}^{*})\underline{\underline{I}} \tag{7}$$

$$\underline{\underline{e}}^{*}=\frac{1}{2}[\nabla\underline{d}^{*}+(\nabla\underline{d}^{*})^t] \tag{8}$$

$$\underline{\underline{S}}^{*}=-n_0P^{*(2)}\underline{\underline{I}} \tag{9}$$

$$\rho_{11}=(1-n_0)\rho_s+\rho_a \tag{10}$$

$$\rho_{12}=-\rho_a \tag{11}$$

$$\rho_{22}=n_0\rho_0+\rho_a \tag{12}$$

$$b=\mu n_0^2/k_p \tag{13}$$

where $\underline{\underline{\sigma}}^{*}$=the total stress tensor of solid, $\underline{\underline{\tau}}^{*}$=the effective stress tensor of solid, $\underline{\underline{S}}^{*}$=the normal stress tensor of fluid, $\underline{d}^{*}$ and $\underline{D}^{*}$=the displacements of solid and fluid, respectively, $P^{*(2)}$=the wave-induced pore water pressure, ρ_s=the density of solid, ρ_a=the mass coupling effect (neglected in this study), n_0=the porosity, μ=the viscosity of fluid, k_p=the specific permeability, G and λ=Lame constants of elasticity, and $\underline{\underline{I}}$=the identity matrix.

Combining the continuity equations of solid and fluid with the state equation of fluid and after linearization of the porosity (Verruijt 1969), we can find

$$\frac{\partial P^{*(2)}}{\partial t}=-\frac{K}{n_0}\left[(1-n_0)\nabla\cdot\left(\frac{\partial\underline{d}^{*}}{\partial t}\right)+n_0\nabla\cdot\left(\frac{\partial\underline{D}^{*}}{\partial t}\right)\right] \tag{14}$$

for waved-induced pore water pressure. In Eq. (14), K=the bulk modulus of compressibility of fluid inside the porous bed.

There are three boundaries: (1) free surface $[y=h+\eta^{*}(x,t)]$; (2) porous-bed interface $[y=\xi^{*}(x,t)]$; and (3) poroelastic-bed/impervious rock interface $[y=-B]$ in this study, which, referring to Deresiewicz and Skalak (1963), are required to satisfy the following boundary conditions.

At the free surface, a kinematic boundary condition exists as

$$-\frac{\partial\eta^{*}}{\partial x}\frac{\partial\Phi^{*(1)}}{\partial x}+\frac{\partial\Phi^{*(1)}}{\partial y}=\frac{\partial\eta^{*}}{\partial t} \tag{15}$$

and a dynamic boundary condition exists as

$$\frac{\partial\Phi^{*(1)}}{\partial t}+\frac{1}{2}\left\{\left[\frac{\partial\Phi^{*(1)}}{\partial x}\right]^2+\left[\frac{\partial\Phi^{*(1)}}{\partial y}\right]^2\right\}+g\eta^{*}=0 \tag{16}$$

At the porous-bed surface, the continuity of pressure for fluid gives

$$P^{*(1)}=P^{*(2)} \tag{17}$$

and the continuity of fluid flux gives

$$\underline{n}_2^{*}\cdot\left[(1-n_0)\frac{\partial\underline{d}^{*}}{\partial t}+n_0\frac{\partial\underline{D}^{*}}{\partial t}\right]=\underline{n}_2^{*}\cdot\nabla\Phi^{*(1)} \tag{18}$$

where

$$\underline{n}_2^{*}=\left(\frac{-\partial\xi^{*}}{\partial x},1\right)\Bigg/\sqrt{1+\left(\frac{\partial\xi^{*}}{\partial x}\right)^2} \tag{19}$$

is the unit normal vector at the porous bed surface. Considering the kinematics of this surface, we have

$$\frac{\partial\xi^{*}}{\partial t}=\frac{\partial\underline{d}^{*}}{\partial t}\cdot\left(-\frac{\partial\xi^{*}}{\partial x},1\right) \tag{20}$$

and Eq. (20) will be used to solve ξ^{*}. And the continuity of effective stresses of solid gives

$$\underline{n}_2^{*}\cdot\underline{\underline{\tau}}^{*}=\underline{0} \tag{21}$$

At the interface between the porous bed and the impervious rock, $y=-B$, the boundary conditions are no displacement for porous material

$$\underline{d}^{*}=\underline{0} \tag{22}$$

and no flux for fluid

$$\underline{u}_{2y}^{*}=0 \tag{23}$$

where $\underline{u}_{2y}^{*}$=the vertical component of the velocity of fluid within the porous bed.

If both $|\eta^{*}|$ and $|\xi^{*}|$ are much smaller than the relative wavelengths, it is more convenient to shift the boundary conditions at the free surface, $y=h+\eta^*(x,t)$, and at the porous bed surface, $y=\xi^*(x,t)$, to $y=h$ and $y=0$ first before solving the boundary-value problem. Conventionally, Taylor series expansions are applied to the boundary conditions at the free surface [Eqs. (15) and (16)] and at the porous bed surface [Eqs. (17), (18), (21), and (20)] by performing

$$\sum_{m=0}^{\infty} \frac{(\eta^*)^m}{m!} \frac{\partial^m}{\partial y^m} \quad \text{and} \quad \sum_{m=0}^{\infty} \frac{(\xi^*)^m}{m!} \frac{\partial^m}{\partial y^m}$$

respectively, before liquefaction.

As will be indicated by Eq. (39), for the present problem, due to the existence of the second longitudinal wave (with wave number k_2) inside the boundary layer of the soft poroelastic bed, the aforementioned Taylor series expansions at the interface $(y=0)$ are applicable for the first longitudinal wave (with wave number k_1) and the transverse wave (with wave number k_3), but not applicable for the second longitudinal wave because the effect of the boundary layer will render errors of the partial derivative in the vertical direction for the second longitudinal wave. That is why Chen et al. (1997) failed to solve the nonlinear problem for soft porous material by only one length scale. To overcome the difficulty, another small parameter $\varepsilon_2=k_0/k_2$, other than $\varepsilon_1=k_0 a$, needs to be proposed. Thus, the vertical coordinate y for the second longitudinal wave will be enlarged into y' based on this small parameter ε_2 [see Eq. (43*b*)].

Referring to Huang and Song (1993) for the decoupling processes of Biot's equations of poroelasticity (1956), governing Eqs. (4) and (5) can be rewritten into three decoupled scalar equations as

$$\nabla^2\Phi_j^{*(2)}+k_j^2\Phi_j^{*(2)}=0, \quad j=1,2,3 \tag{24}$$

Also, Eq. (14) of the wave-induced pore water pressure gives

$$P^{*(2)}=\frac{K}{n_0}[(1-n_0+\alpha_1 n_0)k_1^2\Phi_1^{*(2)}+(1-n_0+\alpha_2 n_0)k_2^2\Phi_2^{*(2)}] \tag{25}$$

where wave numbers k_j and solid/fluid related parameters α_j are given as Eqs. (8)–(20) in Huang and Song (1993). In Eq. (24), $\Phi_1^{(2)}$ and $\Phi_2^{(2)}$=the displacement potentials of the first and the second longitudinal waves, respectively; while $\Phi_3^{(2)}$=the displacement potential of the transverse wave, i.e.

$$\underset{\sim}{d}^*=\nabla\Phi_1^{*(2)}+\nabla\Phi_2^{*(2)}+\nabla\wedge(\Phi_3^{*(2)}\underset{\sim}{e}_z) \tag{26}$$

$$\underset{\sim}{D}^*=\alpha_1\nabla\Phi_1^{*(2)}+\alpha_2\nabla\Phi_2^{*(2)}+\alpha_3\nabla\wedge(\Phi_3^{*(2)}\underset{\sim}{e}_z) \tag{27}$$

In which, $\nabla\wedge(\ )$ means taking curl of ( ).

Note that governing Eqs. (2) and (24), wave-induced pressure and effective stresses Eqs. (3), (25), and (7), together with boundary conditions (15), (16), (17), (18), (21), (22), and (23) form the complete boundary-value problem of the present study. [Eq. (20) is used to find ξ^* only, and the vertical component of Eq. (22) is identical to Eq. (23) in the present study.]

Nondimensionalization of Variables

Huang and Song (1993) defined the following parameters

$$m=(2G+\lambda)n_0/K \tag{28}$$

$$\varepsilon=n_0\rho_0\omega/b \tag{29}$$

$$\Lambda^2=\frac{n_0\rho_0+(1-n_0)\rho_s}{2G+\lambda+(K/n_0)}\frac{\omega^2}{k_0^2} \tag{30}$$

$$\Pi^2=\frac{i(m+1)}{m\varepsilon}\frac{\rho_0}{K}\frac{\omega^2}{k_0^2} \tag{31}$$

$$\Psi^2=\frac{n_0\rho_0+(1-n_0)\rho_s}{G}\frac{\omega^2}{k_0^2} \tag{32}$$

in their solution of linear water waves propagating over a poroelastic bed. In which, ε=called penetrability parameter, ω=the frequency, m=the stiffness ratio of solid and fluid, k_0=the wave number of water wave and will be found as complex, Λ and Ψ are only functions of water wave speed and material (fluid and solid skeleton) properties, while Π is not only a function of the same variables for Λ and Ψ but also depends on the permeability of the porous medium.

Referring to Huang and Chwang (1990), k_1, k_2, and k_3 can be derived in the following form:

$$k_1=\left[\frac{n_0\rho_0+(1-n_0)\rho_s}{2G+\lambda+(K/n_0)}\right]^{1/2}\omega[1+O(\varepsilon)] \tag{33}$$

$$k_2=\left[\frac{2G+\lambda+(K/n_0)}{(2G+\lambda)n_0K}i\omega b\right]^{1/2}[1+O(\varepsilon)] \tag{34}$$

$$k_3=\left[\frac{n_0\rho_0+(1-n_0)\rho_s}{G}\right]^{1/2}\omega[1+O(\varepsilon)] \tag{35}$$

For low penetrability, i.e., $\|\varepsilon\|\ll 1$, Eqs. (30)–(32) could be simplified to

$$\Lambda^2 \doteqdot (k_1/k_0)^2 \tag{36}$$

$$\Pi^2 \doteqdot (k_2/k_0)^2 \tag{37}$$

$$\Psi^2 \doteqdot (k_3/k_0)^2 \tag{38}$$

by substitution of Eqs. (33)–(35). Moreover, for a soft solid skeleton, $\|k_2\|\gg\|k_0\|$ is discovered and that $\|\Pi^2\|\doteqdot\|k_2^2/k_0^2\|\gg 1$ is used to define the "soft" material in this study. Since $\|\Lambda^2\|$ is always smaller than $\|\Psi^2\|$ [see Eqs. (30) and (32)], we can obtain

$$\|\Lambda^2\|<\|\Psi^2\|\ll 1\ll\|\Pi^2\| \tag{39}$$

Based on the this discussion, we herewith define

$$\varepsilon_1=k_0 a \tag{40}$$

$$\varepsilon_2=k_0/k_2 \tag{41}$$

for later use where a=the amplitude of an incoming water wave.

After the analysis of an order of magnitude for each dependent variable, the dimensionless variables are selected as

$$\hat{x}=k_0 x \tag{42}$$

$$\hat{y}=k_0 y \tag{43a}$$

$$y'=\hat{y}/\varepsilon_2, \quad \text{for the second longitudinal wave only} \tag{43b}$$

$$\hat{t}=\sqrt{gk_0}\,t \tag{44}$$

$$\hat{\eta}^*=k_0\eta^* \tag{45}$$

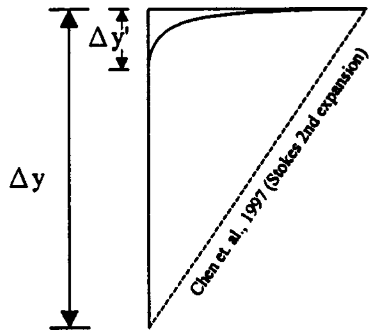

Fig. 2. Schematic diagram of vertical length scales inside boundary layer for second longitudinal wave

$$\hat{\omega}=\omega/\sqrt{gk_0} \tag{46}$$

$$\hat{\Phi}^{*(1)}=\frac{k_0^2}{\sqrt{gk_0}}\Phi^{*(1)} \tag{47}$$

$$\hat{\Phi}_1^{*(2)}=e^{k_0h}k_0^2\Phi_1^{*(2)} \tag{48}$$

$$\hat{\Phi}_2^{*(2)}=e^{k_0h}k_0^2\frac{k_2^2}{k_1^2}\Phi_2^{*(2)}=\frac{e^{k_0h}k_0^2}{\varepsilon_2^2\Lambda^2}\Phi_2^{*(2)} \tag{49}$$

$$\hat{\Phi}_3^{*(2)}=e^{k_0h}k_0^2\Phi_3^{*(2)} \tag{50}$$

$$\hat{\xi}^{*}=\frac{k_0e^{k_0h}}{\Psi^2}\xi^{*} \tag{51}$$

$$\hat{P}^{*(1)}=\frac{k_0}{\rho_0 g}P^{*(1)} \tag{52}$$

$$\hat{P}^{*(2)}=\frac{k_0}{\rho_0 g}P^{*(2)} \tag{53}$$

All the symbols of variables on the left-hand side of Eqs. (42)–(53) are dimensionless, but those on the right-hand side are dimensional. Note that since vertical length scales need multiple scales (see Fig. 2), $\hat{y}$ and y' are proposed.

Applying the two-parameter perturbation expansion (see Fig. 3), the velocity potential of flow and displacement potentials of the first longitudinal wave and the transverse wave for the whole domain can be written as

$$\hat{\Phi}^{*(1)}=\varepsilon_1\hat{\phi}_{10}^{*}+\varepsilon_1\varepsilon_2\hat{\phi}_{11}^{*}+\varepsilon_1^2\hat{\phi}_{20}^{*}+O(\varepsilon_1^2\varepsilon_2,\ldots) \tag{54}$$

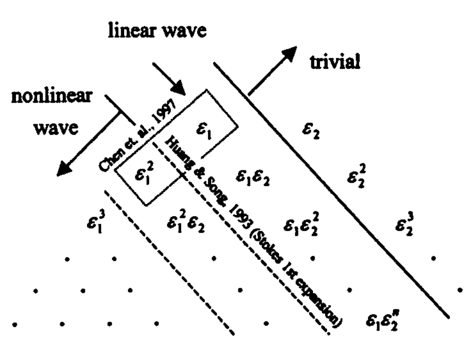

Fig. 3. Schematic diagram of two-parameter expansion

$$\hat{\Phi}_j^{*(2)}=\varepsilon_1\hat{\phi}_{10}^{*[j]}+\varepsilon_1\varepsilon_2\hat{\phi}_{11}^{*[j]}+\varepsilon_1^2\hat{\phi}_{20}^{*[j]}+O(\varepsilon_1^2\varepsilon_2,\ldots),\quad j=1,3 \tag{55}$$

Due to Eq. (39), the second longitudinal wave needs to be solved inside the boundary layer and, thus, its displacement potential is nondimensionalized especially as Eq. (49) and expanded as

$$\hat{\Phi}_2^{*(2)}=\varepsilon_1\hat{\phi}_{10}^{*[2]}+\varepsilon_1\varepsilon_2\hat{\phi}_{11}^{*[2]}+\varepsilon_1^2\hat{\phi}_{20}^{*[2]}+O(\varepsilon_1^2\varepsilon_2,\ldots) \tag{56}$$

if $\|\varepsilon_2\|$ and $\|\varepsilon_1\|$ are smaller than unity. Also, the water wave profile at the free surface becomes

$$\hat{\eta}^{*}=\varepsilon_1\hat{\eta}_{10}^{*}+\varepsilon_1\varepsilon_2\hat{\eta}_{11}^{*}+\varepsilon_1^2\hat{\eta}_{20}^{*}+O(\varepsilon_1^2\varepsilon_2,\ldots) \tag{57}$$

and the wave profile of the porous-bed surface becomes

$$\hat{\xi}^{*}=\varepsilon_1\hat{\xi}_{10}^{*}+\varepsilon_1\varepsilon_2\hat{\xi}_{11}^{*}+\varepsilon_1^2\hat{\xi}_{20}^{*}+O(\varepsilon_1^2\varepsilon_2,\ldots) \tag{58}$$

For a periodic motion with frequency ω, the aforementioned variables $[\ \ ]^*(\underset{\sim}{R},t)$ can be written as $[\ \ ](\underset{\sim}{R})e^{-i\omega t}$, where $\underset{\sim}{R}$=the position vector. Let the given incoming-wave amplitude of the leading order term before being disturbed by the porous bed be a (i.e., $\hat{\eta}_{10}=e^{i\hat{x}}$), the Stokes expansion based on ε_1 and ε_2 will be carried out only to the first three terms for the present nonlinear water wave problem to avoid the occurrence of secular terms. Thus, after the Taylor series expansions at the free surface and at the porous-bed surface, respectively, are applied, the boundary-value problem of each order without the time factor is obtained in the following.

Boundary-Value Problem Without Boundary Layer

Since the first longitudinal wave and the transverse wave propagate throughout the whole domain, i.e., both inside and outside the boundary layer, there is no need to make any corrections of these two waves. Hence, the boundary-value problem without the boundary layer is formulated as follows.

For $O(\varepsilon_1)$, the governing equations are as follows: region (1): $-\infty<\hat{x}<\infty,\ 0<\hat{y}<k_0h$

$$\hat{\nabla}^2\hat{\phi}_{10}=0 \tag{59}$$

and region (2): $-\infty<\hat{x}<\infty,\ -k_0B<\hat{y}<0$

$$\hat{\nabla}^2\hat{\phi}_{10}^{[1]}+\Lambda^2\hat{\phi}_{10}^{[1]}=0 \tag{60}$$

$$\hat{\nabla}^2\hat{\phi}_{10}^{[3]}+\Psi^2\hat{\phi}_{10}^{[3]}=0 \tag{61}$$

the Boundary conditions are as follows; at the free surface: $\hat{y}=k_0h,\ -\infty<\hat{x}<\infty$, (1) kinematic free surface boundary condition

$$\hat{\phi}_{10,\hat{y}}=-i\hat{\omega}\hat{\eta}_{10} \tag{62}$$

and (2) dynamic free surface boundary condition

$$i\hat{\omega}\hat{\phi}_{10}=\hat{\eta}_{10} \tag{63}$$

at the porous-bed surface: $\hat{y}=0,\ -\infty<\hat{x}<\infty$, (1) continuity of pressure

$$i\hat{\omega}\hat{\phi}_{10}-\frac{k_0K\Lambda^2}{e^{k_0h}n_0\rho_0 g}q_1\hat{\phi}_{10}^{[1]}=0 \tag{64}$$

(2) continuity of flux

$$i\hat{\omega}q_1\hat{\phi}_{10,\hat{y}}^{[1]}-i\hat{\omega}q_3\hat{\phi}_{10,\hat{x}}^{[3]}+e^{k_0h}\hat{\phi}_{10,\hat{y}}=0 \tag{65}$$

(3) continuity of effective stress (only $\tau_{\hat{x}\hat{y}}\doteq 0$)

$$2\hat{\phi}^{[1]}_{10,\hat{x}\hat{y}}+\hat{\phi}^{[3]}_{10,\hat{y}\hat{y}}-\hat{\phi}^{[3]}_{10,\hat{x}\hat{x}}=0 \quad (66)$$

at the porous material/impervious rock interface: $\hat{y}=-k_0B$, $-\infty<\hat{x}<\infty$, (1) no horizontal displacement for porous material

$$\hat{\phi}^{[1]}_{10,x}+\hat{\phi}^{[3]}_{10,y}=0 \quad (67)$$

(2) no flux for fluid

$$\alpha_1\hat{\phi}^{[1]}_{10,\hat{y}}-\alpha_3\hat{\phi}^{[3]}_{10,\hat{x}}=0 \quad (68)$$

where

$$q_j=1-n_0+\alpha_j n_0, \quad j=1,3 \quad (69)$$

Note that only one component of the aforementioned boundary conditions of continuity of effective stresses is needed, i.e., $\tau_{\hat{x}\hat{y}}\doteqdot 0$, otherwise, it will become overdetermined. (Another condition, $\tau_{\hat{y}\hat{y}}\doteqdot 0$, includes the effect of the second longitudinal wave and which will be adopted by the boundary layer correction for the second longitudinal wave later.) And, since for the low penetrability of the porous material, both α_1 and α_3 are very close to unity, the boundary condition of no flux for fluid is equivalent to that of no vertical displacement of the soft porous material, therefore, only one is needed. Herein, the former is selected.

For $O(\varepsilon_1\varepsilon_2)$, the governing equations are as follows: region (1): $-\infty<\hat{x}<\infty$, $0<\hat{y}<k_0h$

$$\hat{\nabla}^2\hat{\phi}_{11}=0 \quad (70)$$

region (2): $-\infty<\hat{x}<\infty$, $-k_0B<\hat{y}<0$

$$\hat{\nabla}^2\hat{\phi}^{[1]}_{11}+\Lambda^2\hat{\phi}^{[1]}_{11}=0 \quad (71)$$

$$\hat{\nabla}^2\hat{\phi}^{[3]}_{11}+\Psi^2\hat{\phi}^{[3]}_{11}=0 \quad (72)$$

The boundary conditions are the following at the free surface: $\hat{y}=k_0h$, $-\infty<\hat{x}<\infty$ (1) kinematic free surface boundary condition

$$\hat{\phi}_{11,\hat{y}}=-i\hat{\omega}\hat{\eta}_{11} \quad (73)$$

(2) dynamic free surface boundary condition

$$i\hat{\omega}\hat{\phi}_{11}=\hat{\eta}_{11} \quad (74)$$

at the porous-bed surface: $\hat{y}=0$, $-\infty<\hat{x}<\infty$, (1) continuity of pressure

$$i\hat{\omega}\hat{\phi}_{11}-\frac{k_0K\Lambda^2}{e^{k_0h}n_0\rho_0 g}q_1\hat{\phi}^{[1]}_{11}=0 \quad (75)$$

(2) continuity of flux

$$i\hat{\omega}e^{-k_0h}(q_1\hat{\phi}^{[1]}_{11,\hat{y}}-q_3\hat{\phi}^{[3]}_{11,\hat{x}})+\hat{\phi}_{11,\hat{y}}=0 \quad (76)$$

(3) continuity of effective stress (only $\tau_{\hat{x}\hat{y}}\doteqdot 0$)

$$2\hat{\phi}^{[1]}_{11,\hat{x}\hat{y}}+\hat{\phi}^{[3]}_{11,\hat{y}\hat{y}}-\hat{\phi}^{[3]}_{11,\hat{x}\hat{x}}=0 \quad (77)$$

at the porous material/impervious rock interface: $\hat{y}=-k_0B$, $-\infty<\hat{x}<\infty$ (1) no horizontal displacement for porous material

$$\hat{\phi}^{[1]}_{11,\hat{x}}+\hat{\phi}^{[3]}_{11,\hat{y}}=0 \quad (78)$$

(2) no flux for fluid

$$\alpha_1\hat{\phi}^{[1]}_{11,\hat{y}}-\alpha_3\hat{\phi}^{[3]}_{11,\hat{x}}=0 \quad (79)$$

Again, only one component of the boundary condition of continuity of effective stresses is needed, i.e., $\tau_{\hat{x}\hat{y}}\doteqdot 0$, for the same reason mentioned herein, and the vanishing vertical solid displacement is equivalent to vanishing fluid flux at impervious boundary.

For $O(\varepsilon_1^2)$, the governing equations are as follows: region (1): $-\infty<\hat{x}<\infty$, $0<\hat{y}<k_0h$

$$\hat{\nabla}^2\hat{\phi}_{20}=0 \quad (80)$$

region (2): $-\infty<\hat{x}<\infty$, $-k_0B<\hat{y}<0$

$$\hat{\nabla}^2\hat{\phi}^{[1]}_{20}+\frac{\tilde{k}_1^2}{k_1^2}\Lambda^2\hat{\phi}^{[1]}_{20}=0 \quad (81)$$

$$\hat{\nabla}^2\hat{\phi}^{[3]}_{20}+\frac{\tilde{k}_3^2}{k_3^2}\Psi^2\hat{\phi}^{[3]}_{20}=0 \quad (82)$$

The boundary conditions are as follows: at the free surface: $\hat{y}=k_0h$, $-\infty<\hat{x}<\infty$, (1) kinematic free surface boundary condition

$$\hat{\phi}_{20,\hat{y}}+2i\hat{\omega}\hat{\eta}_{20}=\hat{\eta}_{10,\hat{x}}\hat{\phi}_{10,\hat{x}}-\hat{\eta}_{10}\hat{\phi}_{10,\hat{y}\hat{y}} \quad (83)$$

(2) dynamic free surface boundary condition

$$2i\hat{\omega}\hat{\phi}_{20}-\hat{\eta}_{20}=\frac{1}{2}(\hat{\phi}^2_{10,\hat{x}}+\hat{\phi}^2_{10,\hat{y}})-i\hat{\omega}\hat{\eta}_{10}\hat{\phi}_{10,\hat{y}} \quad (84)$$

at the porous-bed surface: $\hat{y}=0$, $-\infty<\hat{x}<\infty$, (1) continuity of pressure

$$2i\hat{\omega}\hat{\phi}_{20}-\frac{k_0K\Lambda^2}{e^{k_0h}n_0\rho_0 g}\tilde{q}_1\hat{\phi}^{[1]}_{20}=\frac{1}{2}(\hat{\phi}^2_{10,\hat{x}}+\hat{\phi}^2_{10,\hat{y}})-\frac{i\hat{\omega}\Psi^2\hat{\xi}_{10}}{e^{k_0h}}\hat{\phi}_{10,\hat{y}}+\frac{\Psi^2k_0K\Lambda^2\hat{\xi}_{10}}{e^{2k_0h}n_0\rho_0 g}q_1\hat{\phi}^{[1]}_{10,\hat{y}} \quad (85)$$

(2) continuity of flux

$$e^{k_0h}\hat{\phi}_{20,\hat{y}}+2i\hat{\omega}(\tilde{q}_1\hat{\phi}^{[1]}_{20,\hat{y}}-\tilde{q}_3\phi^{[3]}_{20,\hat{x}})=\Psi^2\hat{\xi}_{10,\hat{x}}\hat{\phi}_{10,\hat{x}}-\Psi^2\hat{\xi}_{10}\hat{\phi}_{10,\hat{y}\hat{y}}+i\hat{\omega}\Psi^2e^{-k_0h}\hat{\xi}_{10,\hat{x}}(q_1\hat{\phi}^{[1]}_{10,\hat{x}}+q_3\hat{\phi}^{[3]}_{10,\hat{y}})-i\hat{\omega}\Psi^2e^{-k_0h}\hat{\xi}_{10}(q_1\hat{\phi}^{[1]}_{10,\hat{y}\hat{y}}-q_3\hat{\phi}^{[3]}_{10,\hat{y}\hat{x}}) \quad (86)$$

(3) continuity of effective stress (only $\tau_{\hat{x}\hat{y}}\doteqdot 0$)

$$G(2\hat{\phi}^{[1]}_{20,\hat{x}\hat{y}}+\hat{\phi}^{[3]}_{20,\hat{y}\hat{y}}-\hat{\phi}^{[3]}_{20,\hat{x}\hat{x}})=\Psi^2e^{-k_0h}\hat{\xi}_{10,\hat{x}}[2G(\hat{\phi}^{[1]}_{10,\hat{x}\hat{x}}+\hat{\phi}^{[3]}_{10,\hat{x}\hat{y}})-\lambda\Lambda^2\hat{\phi}^{[1]}_{10}]-G\Psi^2e^{-k_0h}\hat{\xi}_{10}(2\hat{\phi}^{[1]}_{10,\hat{x}\hat{y}\hat{y}}+\hat{\phi}^{[3]}_{10,\hat{y}\hat{y}\hat{y}}-\hat{\phi}^{[3]}_{10,\hat{x}\hat{x}\hat{y}}) \quad (87)$$

at the porous material/impervious rock interface: $\hat{y}=-k_0B$, $-\infty<\hat{x}<\infty$, (1) no horizontal displacement for porous material

$$\hat{\phi}^{[1]}_{20,\hat{x}}+\hat{\phi}^{[3]}_{20,\hat{y}}=0 \quad (88)$$

(2) no flux for fluid

$$\alpha_1\hat{\phi}^{[1]}_{20,\hat{y}}-\alpha_3\hat{\phi}^{[3]}_{20,\hat{x}}=0 \quad (89)$$

where $\tilde{k}_j$ and $\tilde{\alpha}_j$ $(j=1,3)$ in nonlinear order ε_1^2 are given as Eqs. (8)–(20) in Huang and Song (1993), and

$$\tilde{q}_j=1-n_0+\tilde{\alpha}_j n_0, \quad j=1,3 \quad (90)$$

Table 1. Selection of Wave Condition and Property of Soft Porous Bed

Item	Value	Unit
	Water	
Density	1,000	kg/m^3
Bulk modulus	2.3×10^9	N/m^2
Viscosity	0.001	N s/m^2
Depth	2.0	m
Wave amplitude	0.05	m
Period	2.0	s
	Skeleton	
Density	2,650	kg/m^3
Lame's constant	1.0×10^6	N/m^2
Lame's constant	1.0×10^7	N/m^2
Specific permeability	1.0×10^{-12}	m^2
Porosity	0.4	

Boundary Layer Correction Inside Boundary Layer

The second longitudinal wave disappears outside the boundary layer but it does exist inside the boundary layer near the water/porous-bed interface, so the complete solution needs to be corrected by further consideration of the second longitudinal wave inside the porous material. Besides, due to the fact that this second longitudinal wave is trapped inside the boundary layer near the water/porous-bed interface, it could not transmit throughout the porous material bed to the interface between the porous material and the impervious rock. In other words, there exists no boundary layer near the porous material/impervious rock interface due to the deficiency of the second longitudinal wave and where only the first longitudinal wave and the transverse wave exist.

Since a thin boundary layer exists within the porous bed near the water/porous-bed interface, multiple scales are needed to solve the nonlinear boundary-value problem for the second longitudinal wave (see Fig. 2). We, therefore, let $y'=\hat{y}/\varepsilon_2$ to change the scale from $\hat{y}$ to the magnified scale y' in (43b). The difficulty that Chen et al. (1997) encountered, the error due to the first partial derivative based on y of the displacement potential of the second longitudinal wave, is now overcome by proposing two length scales in the vertical direction. After the coordinate transformation of (43b), the boundary-value problem of the displacement potential of the second longitudinal wave inside the boundary layer becomes $O(\varepsilon_1)$.

The governing equations are:

$$\hat{\phi}^{[2]}_{10,y'y'}+\hat{\phi}^{[2]}_{10}=0 \tag{91}$$

The boundary conditions: $y'=0,\ -\infty<\hat{x}<\infty$, (1) continuity of vertical effective stress (only $\tau_{\hat{y}\hat{y}}\doteqdot 0$)

$$2G\Lambda^2\hat{\phi}^{[2]}_{10,y'y'}-\lambda\Lambda^2\hat{\phi}^{[2]}_{10}=\lambda\Lambda^2\hat{\phi}^{[1]}_{10}-2G(\hat{\phi}^{[1]}_{10,\hat{y}\hat{y}}-\hat{\phi}^{[3]}_{10,\hat{x}\hat{y}}) \tag{92}$$

(2) outside the boundary layer

$$\hat{\phi}^{[2]}_{10}=0 \tag{93}$$

For $O(\varepsilon_1\varepsilon_2)$, the governing equations are:

$$\hat{\phi}^{[2]}_{11,y'y'}+\hat{\phi}^{[2]}_{11}=0 \tag{94}$$

The boundary conditions: $y'=0,\ -\infty<\hat{x}<\infty$, (1) continuity of vertical effective stress (only $\tau_{\hat{y}\hat{y}}\doteqdot 0$)

$$2G\Lambda^2\hat{\phi}^{[2]}_{11,y'y'}-\lambda\Lambda^2\hat{\phi}^{[2]}_{11}=\lambda\Lambda^2\hat{\phi}^{[1]}_{11}-2G(\hat{\phi}^{[1]}_{11,\hat{y}\hat{y}}-\hat{\phi}^{[3]}_{11,\hat{x}\hat{y}}) \tag{95}$$

(2) outside the boundary layer

$$\hat{\phi}^{[2]}_{11}=0 \tag{96}$$

For $O(\varepsilon_1^2)$, the governing equations are:

$$\hat{\phi}^{[2]}_{20,y'y'}+\hat{\phi}^{[2]}_{20}=0 \tag{97}$$

The boundary conditions: $y'=0,\ -\infty<\hat{x}<\infty$, (1) continuity of vertical effective stress (only $\tau_{\hat{y}\hat{y}}\doteqdot 0$)

$$\begin{aligned}2G\Lambda^2\hat{\phi}^{[2]}_{20,y'y'}-\lambda\Lambda^2\hat{\phi}^{[2]}_{20}\\ &=-2G(\hat{\phi}^{[1]}_{20,\hat{y}\hat{y}}-\hat{\phi}^{[3]}_{20,\hat{x}\hat{y}})+\lambda\Lambda^2\hat{\phi}^{[1]}_{20}-\Psi^2\hat{\xi}_{10}e^{-k_0h}\\ &\quad\times[2G(\hat{\phi}^{[1]}_{10,\hat{y}\hat{y}\hat{y}}+\Lambda^2\hat{\phi}^{[2]}_{11,y'y'y'}-\hat{\phi}^{[3]}_{10,\hat{x}\hat{y}\hat{y}})\\ &\quad-\lambda\Lambda^2(\hat{\phi}^{[1]}_{10,\hat{y}}+\hat{\phi}^{[2]}_{11,y'})]\end{aligned} \tag{98}$$

(2) outside the boundary layer

$$\hat{\phi}^{[2]}_{20}=0 \tag{99}$$

Solution

After omitting the time factor $e^{-i\omega t}$, the given the leading order incoming water wave profile with magnitude a is

$$\eta_{10}(x)=ae^{ik_0x}\quad(0<x<\infty) \tag{100}$$

With the input of the leading order incoming water wave, each order of the aforementioned boundary-value problems can be solved in sequence. Thus, the dimensional solutions of the first longitudinal wave and the transverse wave throughout the entire domain are obtained as follows for $O(\varepsilon_1)$

$$\phi_{10}=-\frac{i}{k_0}\left[\frac{g}{\omega}\cosh k_0(h-y)-\frac{\omega}{k_0}\sinh k_0(h-y)\right]e^{ik_0x} \tag{101}$$

$$\phi^{[1]}_{10}=\frac{1}{e^{k_0h}k_0^2}(a_{11}e^{K_1k_0y}+a_{12}e^{-K_1k_0y})e^{ik_0x} \tag{102}$$

$$\phi^{[3]}_{10}=\frac{1}{e^{k_0h}k_0^2}(a_{31}e^{K_3k_0y}+a_{32}e^{-K_3k_0y})e^{ik_0x} \tag{103}$$

For $O(\varepsilon_1\varepsilon_2)$

$$\phi_{11}=\frac{\sqrt{gk_0}}{k_0^2}E_5\left[\cosh k_0(h-y)-\frac{\omega^2}{gk_0}\sinh k_0(h-y)\right]e^{ik_0x} \tag{104}$$

$$\phi^{[1]}_{11}=\frac{1}{e^{k_0h}k_0^2}(c_{11}e^{K_1k_0y}+c_{12}e^{-K_1k_0y})e^{ik_0x} \tag{105}$$

$$\phi^{[3]}_{11}=\frac{1}{e^{k_0h}k_0^2}(c_{31}e^{K_3k_0y}+c_{32}e^{-K_3k_0y})e^{ik_0x} \tag{106}$$

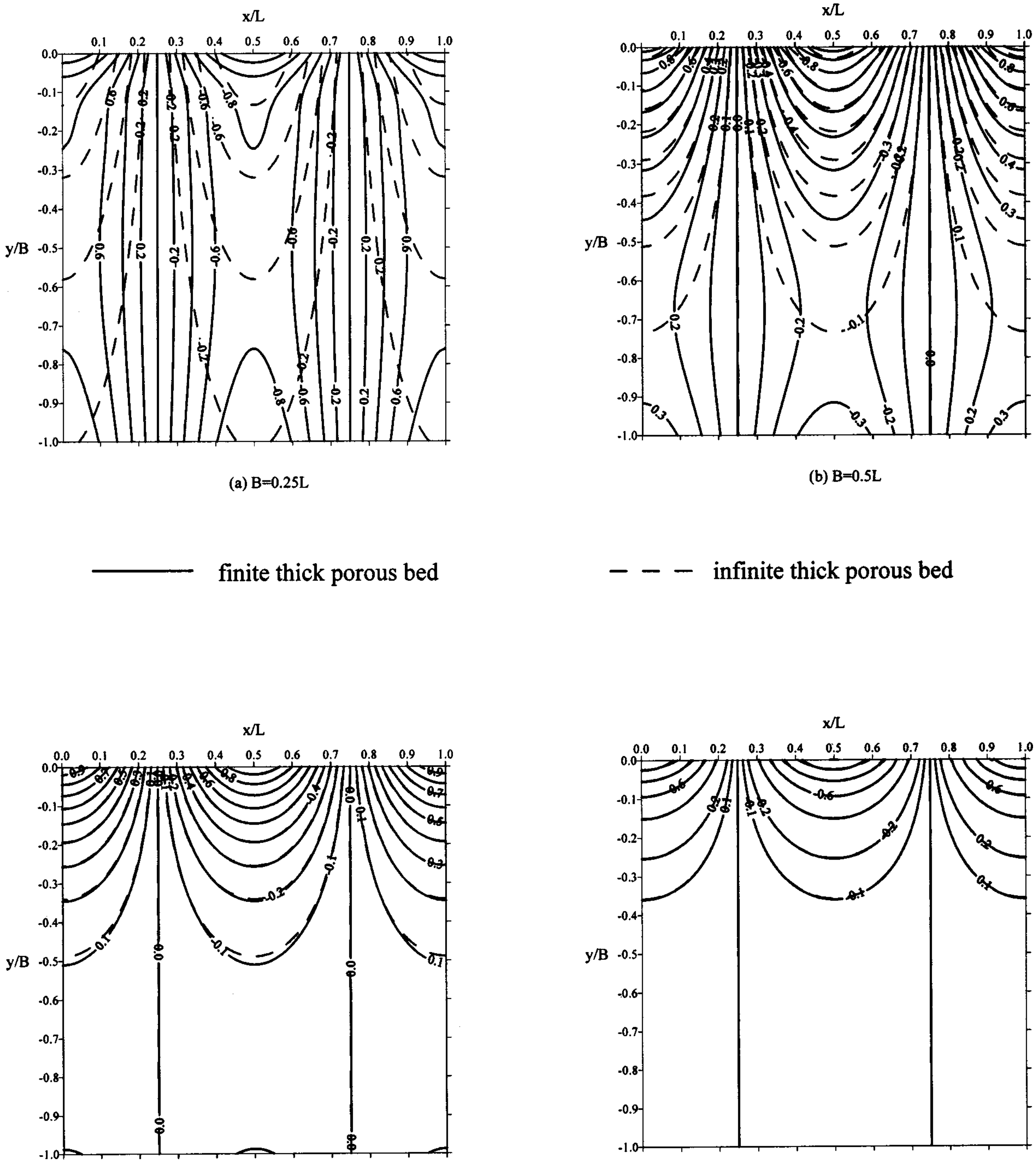

Fig. 4. Distribution of wave-induced pore water pressures $|P^{(2)}/P_0|$

$$\eta_{11}=\frac{i}{k_0}\frac{\omega}{\sqrt{gk_0}}E_5 e^{ik_0x} \tag{107}$$

For $O(\varepsilon_1^2)$

$$\phi_{20}=\frac{\sqrt{gk_0}}{k_0^2}[E_3\cosh 2k_0(h-y)+E_4\sinh 2k_0(h-y)]e^{2ik_0x} \tag{108}$$

$$\phi_{20}^{[1]}=\frac{1}{e^{k_0h}k_0^2}(b_{11}e^{M_1k_0y}+b_{12}e^{-M_1k_0y})e^{2ik_0x} \tag{109}$$

$$\phi_{20}^{[3]}=\frac{1}{e^{k_0h}k_0^2}(b_{31}e^{M_3k_0y}+b_{32}e^{-M_3k_0y})e^{2ik_0x} \tag{110}$$

$$\eta_{20}=\left(\frac{g}{\omega^2}-\frac{iE_4}{\omega k_0}\sqrt{gk_0}\right)e^{2ik_0x} \tag{111}$$

The dimensional solutions of the second longitudinal wave obtained by the boundary layer correction approach for $O(\varepsilon_1)$ is

$$\phi_{10}^{[2]}=\frac{1}{e^{k_0h}k_0^2}\frac{k_1^2}{k_2^2}(a_{21}e^{iy'}+a_{22}e^{-iy'})e^{ik_0x} \tag{112}$$

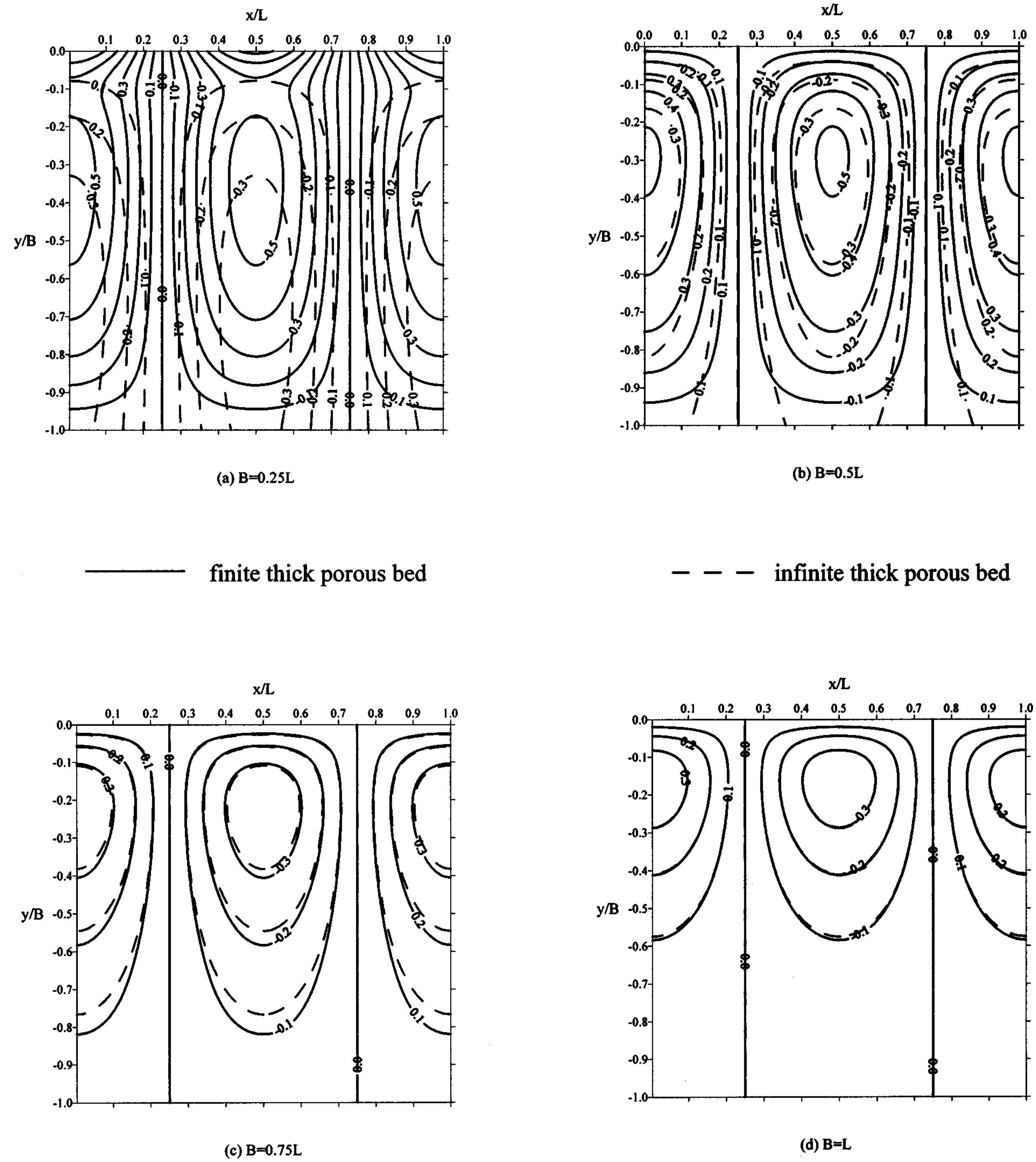

Fig. 5. Distribution of wave-induced horizontal effective stresses $|\tau_{xx}/P_0|$

for $O(\varepsilon_1\varepsilon_2)$ is

$$\phi_{11}^{[2]}=\frac{1}{e^{k_0h}k_0^2}\frac{k_1^2}{k_2^2}(c_{21}e^{iy'}+c_{22}e^{-iy'})e^{ik_0x} \tag{113}$$

and for $O(\varepsilon_1^2)$ is

$$\phi_{20}^{[2]}=\frac{1}{e^{k_0h}k_0^2}\frac{k_1^2}{k_2^2}(b_{21}e^{iy'}+b_{22}e^{-iy'})e^{ik_0x} \tag{114}$$

Since the solutions of the coefficients such as a_{11}, a_{12}, a_{21}, a_{22}, b_{11}, b_{12}, b_{21}, b_{22}, c_{21}, $E_3,\ldots,$ etc. are in a very long and complicated form, they are omitted herein. However, the solutions could be obtained by mathematical tools, e.g., *MATHEMATICA*. After solving the displacement potentials, all the other variables can be obtained. The wave profile of the porous-bed surface can be found from Eqs. (20) and (58).

Results and Comments

Since the second longitudinal wave decays very quickly in the vertical direction inside the boundary layer as shown in Fig. 2, a stretched coordinate is needed to better estimate the partial derivative of the second longitudinal wave. Herein, the present solutions are valid under the constraint of $\|\varepsilon_1\|^{1/2}>\|\varepsilon_2\|>\|\varepsilon_1\|^2$ before liquefaction when referring to Fig. 3.

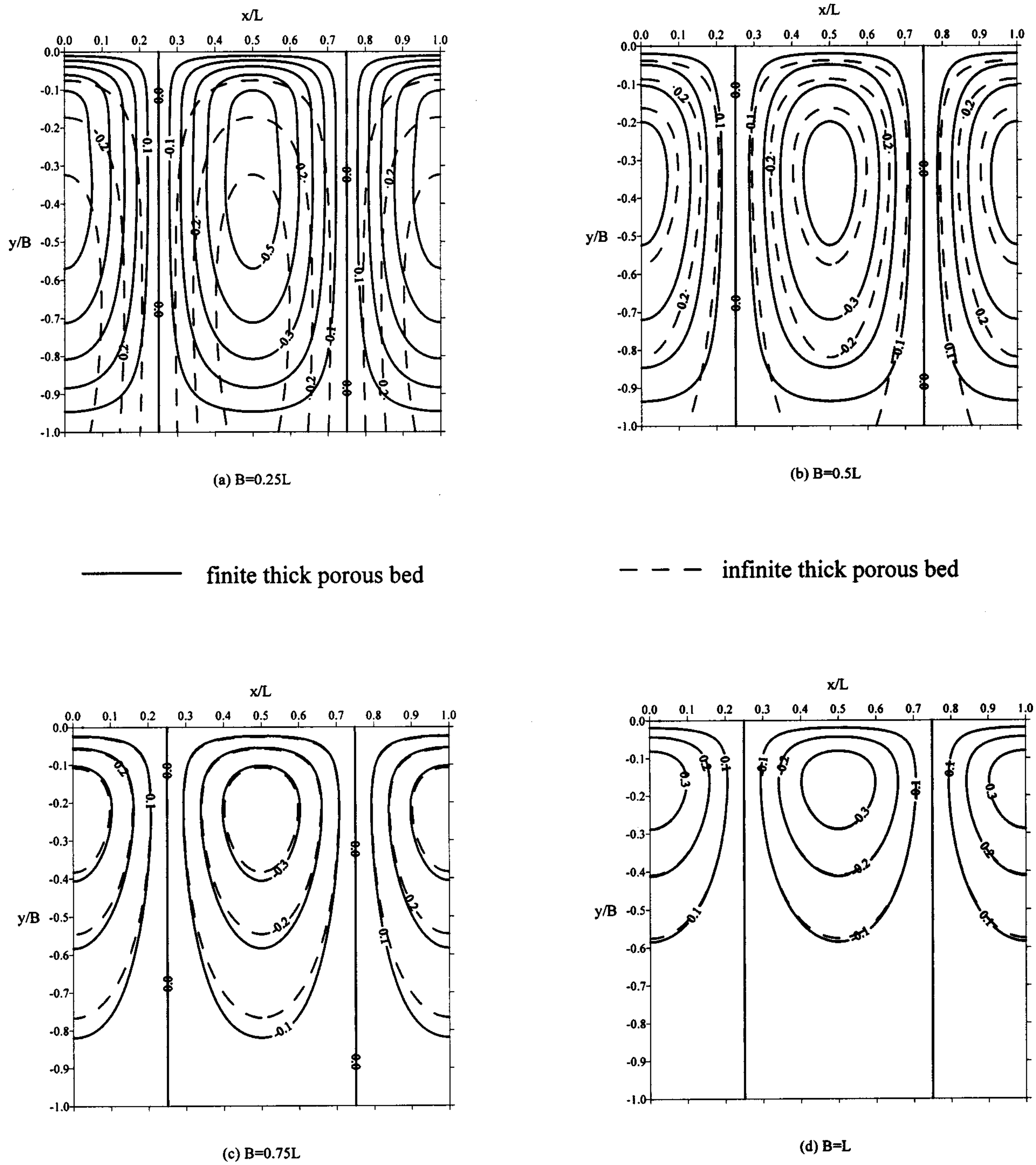

Fig. 6. Distribution of wave-induced vertical effective stresses $|\tau_{yy}/P_0|$

Table 1 gives the wave condition and the material property of a soft bed. The present results are compared with those of the similar problem with infinite thickness provided by Hsieh et al. (2000) to confirm the validity. The two small parameters $(\|\varepsilon_1\|,\|\varepsilon_2\|)$ are found to be (0.052,0.064) by Eqs. (40) and (41) with complex $k_2=(0.161972E+02,0.161970E+02)$, which satisfy the constraint $\|\varepsilon_1\|^{1/2}>\|\varepsilon_2\|>\|\varepsilon_1\|^2$. The complex wave number k_0 is found to be (0.103848E+01,0.184387E−06) and thus the wavelength L is 6.05 m.

Fig. 4 shows the distribution of wave-induced pore water pressures under four different thickness. The solid lines in Fig. 4 denote the present case of finite thick porous bed while the dashed ones denote the case of infinite thick porous bed. These two sets of lines tell that the boundary effect is significant, which feeds pore pressures back into the poroelastic bed very obviously especially when the thickness (B) is less than the half wavelength ($L/2$). The pore pressures become very large at the top and the bottom of the porous bed in Figs. 4(a and b). P_0 in Fig. 4 is the wave-induced water pressure on the mean bed surface ($y=0$), and the nondimensional base B for infinite-thickness case is adopted as the same as in finite-thickness case.

In Fig. 5, the wave-induced horizontal effective stresses of finite-thickness case are larger than those of infinite-thickness case when the thickness is less than the three-fourth wavelength. Besides, this effective stress is influenced obviously by the rigid boundary especially near the top of the porous bed for the case of

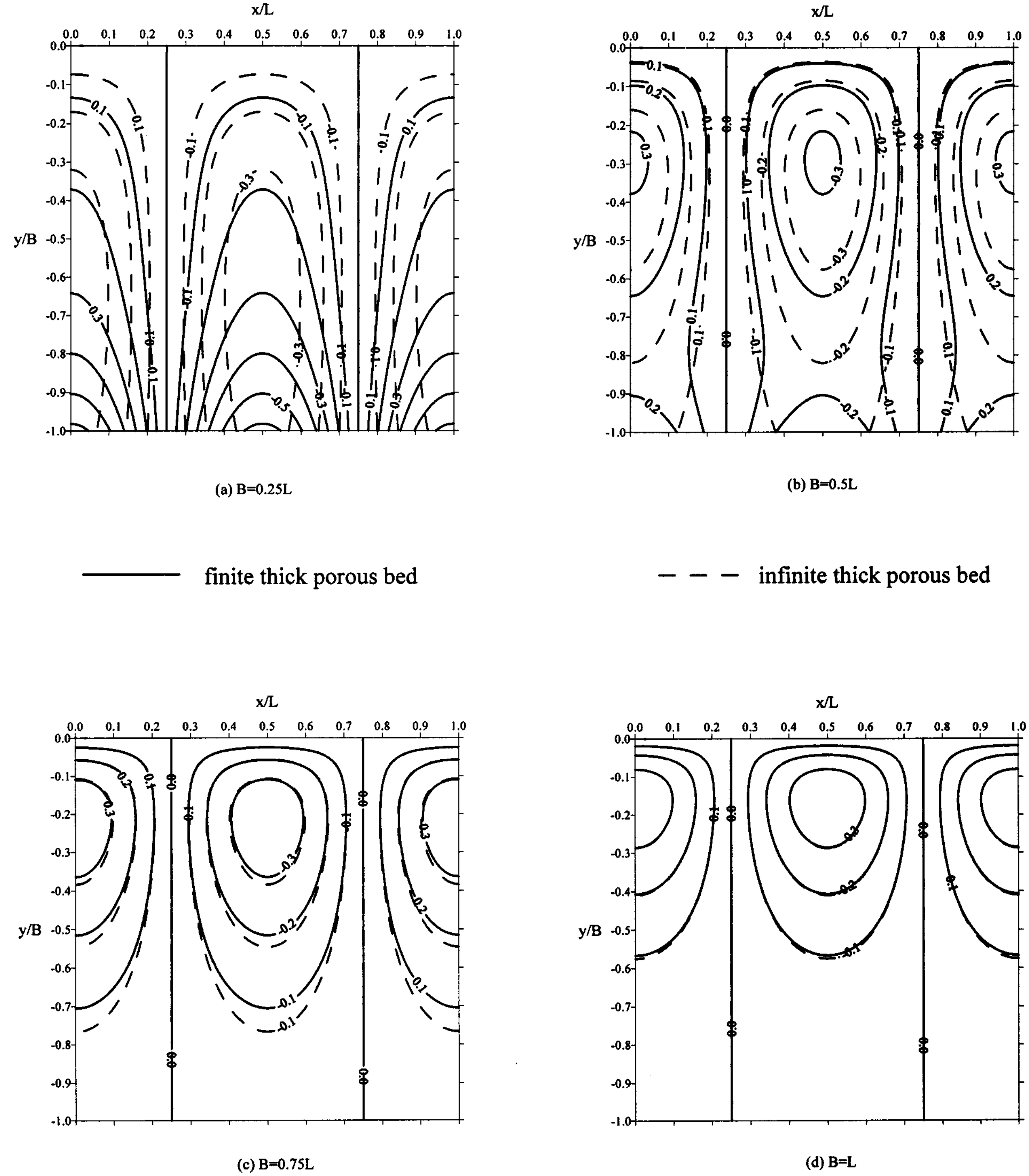

Fig. 7. Distribution of wave-induced shear stresses $|\tau_{xy}/P_0|$

Fig. 5(a). The vertical effective stresses in Fig. 6 are similar to those of Fig. 5.

In Fig. 7, the shear stresses are very much affected by the rigid boundary when the thickness is less than the half wavelength. This indicates that the characteristic of shear stresses is totally different from that of normal stresses. In Figs. 8(a and b), the water wave profiles at the free surface change very little because this study is confined to a deepwater wave problem and the given small-amplitude incident waves. However, in Figs. 8(c and d), the wave profiles at the porous bed change very little for different thickness since they are dominated by the second longitudinal wave which is confined inside the boundary layer for a soft porous layer. This can be referred to the work of Hsieh et al. (2000). In their work, we can find that the solution, Eq. (97), of the wave profile at the porous bed indicates the first term on the right-hand side of Eq. (97) contributed by the first longitudinal wave and the third transverse wave canceling each other for a soft porous bed. Fig. 9 shows that the distribution of the pore water pressure varies with the depth under different thicknesses. The locations of occurrence of the wave-induced maximum pore water pressures are also found to be at the top $(y=0)$ or the bottom $(y=-B)$ of the porous bed depending on the thickness of the porous bed. The optimal thickness (B/L) and the maximum pore pressure $(P^{(2)}/P_0)$ for the present example are (0.193,1.42) at the surface

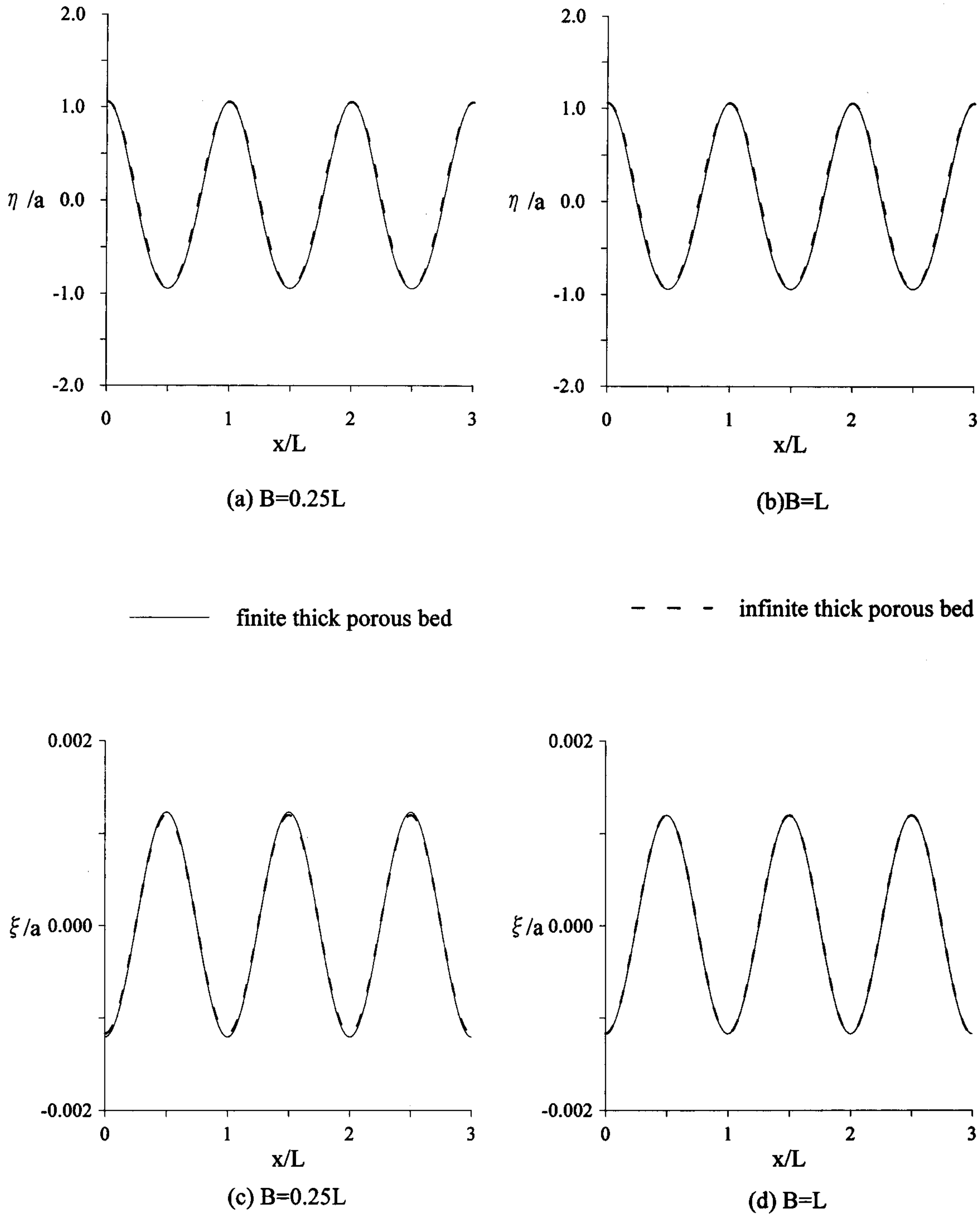

Fig. 8. Wave profiles: (a) and (b) water and (c) and (d) porous bed versus horizontal distance (wave period=2.0 s)

or (0.145,1.13) at the bottom as shown in Fig. 9. If the maximum pore water pressure is large enough to render the occurrence of zero-vertical effective stress by overloading (e.g., the external force due to an earthquake), the porous material is said to be fluidized or liquefied. This surface liquefaction is different from the internal liquefaction of Foda (1987). Although the two sets of contour lines in Fig. 9 are very different in appearance, their values, however, are actually very close when the pore pressures decay under the cases of B/L close to and larger than unity. It is noticeable that for infinite-thickness case the nondimensional base B, which is different from case to case, is chosen as the same one for finite-thickness for each case.

Conclusions

The conventional Stokes expansion of higher-order water waves based on one-parameter $\varepsilon_1 = k_0 a$ is invalid for a soft bed (i.e., $\|\Pi^2\| \doteqdot \|k_2^2/k_0^2\| \gg 1$) with finite thickness because a boundary layer exists inside the porous bed from the second longitudinal wave. Therefore, the boundary layer correction by adopting a two-parameter perturbation expansion based on $\varepsilon_1 = k_0 a$ and $\varepsilon_2 = k_0/k_2$ is proposed and makes the complicated problem possible to be solved by an analytical method other than by a numerical method. Since the porous material bed in nature is usually multi-layered, the present study, which makes the complicated analysis

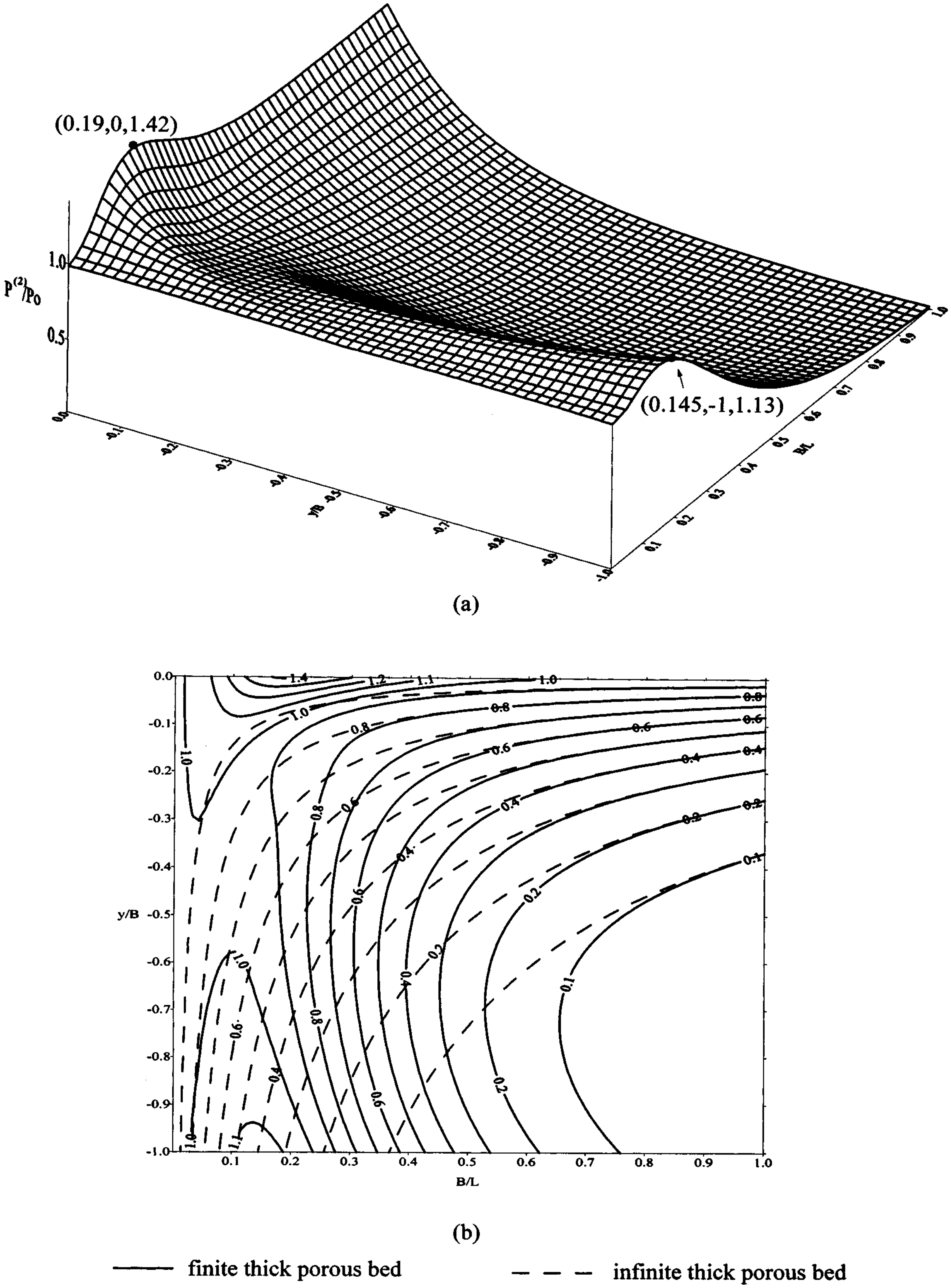

Fig. 9. (a) Three-dimensional variation and (b) contour lines of wave-induced pore water pressures

of the finite-thickness problem possible, is necessary and can be regarded as the first step to further investigations.

The boundary effects of the impervious rock are significant on wave-induced pore water pressure and effective stresses, but not very significant on wave profiles at the free surface and the porous-bed surface. However, the rigid boundary is insignificant to the pore water pressure and effective stresses when the thickness of the porous bed is larger than about one wavelength (see Fig. 9). Furthermore, the peak value of the pore pressure, which is important in analyzing soil liquefaction, could be found if the wave condition and the porous material are given. For example, the locations of maximum pore pressures in the present study occur at either the top or the bottom of the porous bed depending on the thickness of the porous material.

Notation

The following symbols are used in this paper:

a = amplitude of incoming water wave;
$\underline{D}^*$ = displacement of fluid in porous medium;
$\underline{d}^*$ = displacement of solid skeleton;
G, λ = Lame constants of elasticity;
h = mean water depth of the channel;
i = $\sqrt{-1}$;
K = bulk modulus of compressiblity of fluid;
k_j = wave numbers in porous medium, $j=1, 2, 3$;
k_p = specific permeability;
k_0 = wave number of incoming water wave;
n_0 = porosity;
$P^{*(1)}$ = perturbed pressure in channel;
$P^{*(2)}$ = perturbed pressure in porous medium;
P_0 = perturbed pressure on bed;
$\underline{\underline{S}}^*$ = normal stress tensor of fluid;
ε_1 = first expansion parameters of Stokes wave$=k_0 a$;
ε_2 = the second expansion parameters of Stokes wave$=k_0/k_2$;
η^* = displacement of wave deviated from mean-free surface;
Λ,Π,Ψ = Mach numbers of two longitudinal and one transverse waves;
μ = dynamic viscosity of fluid;
ξ^* = displacement of wave deviated from mean channel bed interface;
ρ_0 = density of water;
ρ_s = density of solid;
$\underline{\underline{\sigma}}^*$ = solid stress tensor;
$\underline{\underline{\tau}}^*$ = effective solid stress tensor;
$\Phi^{*(1)}$ = velocity potential of channel flow;
$\Phi_j^{*(2)}$ = jth kind of displacement potentials of porous medium, $j=1, 2, 3$; and
ω = angular frequency of water wave.

References

Biot, M. A. (1956). ‘‘Theory of propagation elastic waves in a fluid saturated porous solid I: Low-frequency range.’’ *JASA*, 28, 168–178.

Chen, T. W., Huang, L. H., and Song, C. H. (1997). ‘‘Dynamic response of poroelastic bed to nonlinear water waves.’’ *J. Eng. Mech.*, 123(10), 1041–1049.

Dean, R. G., and Dalrymple, R. A. (1991). *Water wave mechanics for engineers and scientists*, World Scientific, Singapore.

Deresiewicz, R., and Skalak, R. (1963). ‘‘On uniqueness in dynamic poroelasticity.’’ *Bull. Seismol. Soc. Am.*, 53(4), 783–788.

Fenton, J. D. (1985). ‘‘A fifth-order Stokes theory for steady waves.’’ *J. Waterw., Port, Coastal Ocean Eng. Div., Am. Soc. Civ. Eng.*, 111(2), 216–234.

Foda, M. A. (1987). ‘‘Internal dissipative waves in poroelastic media.’’ *Proc. R. Soc. London, Ser. A*, 413, 383–405.

Hsieh, P. C., Huang, L. H., and Wang, T. W. (2000). ‘‘Dynamic response of soft poroelastic bed to nonlinear water waves—Boundary layer correction approach.’’ *J. Eng. Mech.*, 126(10), 1064–1073.

Huang, L. H., and Chwang, A. T. (1990). ‘‘Trapping and absorption of sound waves. II: Sphere covered with a porous layer.’’ *Wave Motion*, 12, 401–414.

Huang, L. H., and Song, C. H. (1993). ‘‘Dynamic response of poroelastic bed to water waves.’’ *J. Hydraul. Eng.*, 119(9), 1003–1020.

Mei, C. C. (1983). *The applied dynamics of ocean waves*, Wiley, New York.

Moshagen, H., and Torum, A. (1975). ‘‘Wave induced pressures in permeable seabeds.’’ *J. Waterw. Harbors Div., Am. Soc. Civ. Eng.*, 101(1), 49–57.

Putnam, J. A. (1949). ‘‘Loss of wave energy due to percolation in a permeable sea bottom.’’ *Trans., Am. Geophys. Union*, 30, 349–356.

Reid, R. O., and Kajiura, K. (1957). ‘‘On the damping of gravity waves over a permeable sea bed.’’ *Trans., Am. Geophys. Union*, 30, 662–666.

Sleath, J. F. A. (1970). ‘‘Wave induced pressure in bed of sand.’’ *J. Hydraul. Div., Am. Soc. Civ. Eng.*, 96, 367–378.

Verruijt, A. (1969). ‘‘Elastic storage of aquifers.’’ *Flow through porous media*, R. J. M. De DeWiest, ed., Academic, New York.